Investigation of the Formability of Cryogenic Rolled AA6061 and Its Improvement Using Artificial Aging Treatment

Abbas Sadeghi [1,2], Ernst Kozeschnik [2] and Farid R. Biglari [1,*]

1   Mechanical Engineering Department, Amirkabir University of Technology, Tehran 1591634311, Iran
2   Institute of Materials Science and Technology, TU Wien, 1060 Vienna, Austria
*   Correspondence: biglari@aut.ac.ir; Tel.: +98-6454-3434

Abstract: Cryogenic rolling is one of the essential severe plastic deformation processes to manufacture high-strength aluminum sheets with excellent formability limits. The present work characterizes the formability of AA6061 for cryogenic rolling before and after artificial aging. Nakajima method based on ISO standard is used to measure formability. Samples are aged in the range of 100 °C to 150 °C. Artificial aging at 150 °C is found to be the optimum temperature for achieving a good combination of strength and formability. Over the course of artificial aging, strength improved up to 40%, where the original value of 250 MPa for cryo-rolled condition increased to 350 MPa after 50 h of aging at 150 °C, and the formability of the cryo-rolled sample improved especially for multi-axial forming condition.

Keywords: cryogenic rolling; AA6061; forming limit diagram; artificial aging; mechanical properties

1. Introduction

Aluminum alloys are increasingly used due to their light mass, high strength, good reflectivity of heat and light, high corrosion resistance, etc., making them the second most used metal in the world. Aluminum and its alloys are used in electrical power plants, electronic applications, skyscrapers and buildings, aircraft, trains, ships, and personal vehicle components. Using aluminum and its alloys, especially in transportation, can reduce pollution and energy consumption [1,2]. Therefore, improvements in mechanical properties could help their applications. The 6000 series aluminum contains magnesium and silicon as alloying elements and is heat-treatable. A relatively high strength between aluminum alloys and good formability and corrosion resistance extend their application.

Achieving ultrafine-grained (UFG) material is the most prominent key to obtaining better mechanical properties. This requires a severe plastic deformation (SPD) process, such as equal channel angular pressing (ECAP), accumulative roll bonding (ARB), high-pressure torsion (HPT), or cryogenic rolling (CR) [3–7]. Aluminum shows better formability at cryogenic temperatures [8,9], i.e., typically at liquid nitrogen temperature of −196 °C, as more homogeneous plastic deformation of grains occurs [10–12]. Since metals are often used as sheet materials, CR has recently received considerable attention because it can produce continuous industrial products [13–19].

Rolling aluminum in cryogenic temperature suppresses dynamic recovery by reducing dislocation mobility and accumulates dislocation density [13,17,18,20,21]. UFG structures with high dislocation density in sub-grains can be obtained by deformation with large strains below the recrystallization temperature. Moreover, this can increase strain hardening and suppression of strain localization [12,19,22,23].

Post-CR heat treatment results in the precipitation of second phases that are rich in alloying elements. Semi-coherent and coherent precipitates such as β″ and unstable Guinier—Preston (GP) zones are obstacles to dislocation movement so that they can strengthen the material. Therefore, only proper heat treatment can obtain the main strengthening phase in 6xxx series Al alloys, β″ [3,14,24]. Moreover, during post-heat treatment, the

work-hardening effect introduced during cryo-rolling is partially reduced by annihilation and rearrangement of dislocations (recovery). This improves the ductility and reduces the strength of the alloy [24,25].

Consequently, appropriate heat treatment schedules can obtain a suitable combination of strength and ductility. Considering that a large amount of metals is used in sheet form, the formability of sheet metals is of particular interest [15,26,27]. Researchers have addressed several alloys of aluminum in this sense [8,28,29]. Still, there is no report in the literature yet on the forming limit diagram (FLD) of AA6061 subjected to CR and post-heat treatment of age hardening. FLD is one of the best methods to show the formability of sheet metals in different loading conditions. Therefore, in this study, various post-CR heat treatments of AA6061 have been tested, and their corresponding FLDs have been measured to evaluate which heat treatment is more appropriate.

2. Materials and Methods

2.1. Material

AA6061 plates with 10 mm thickness are used as starting point for the present research. The chemical composition of the material is shown in Table 1. The chemical composition is determined with spectroscopy.

Table 1. Chemical composition of the used AA6061 (wt%).

Element	Mg	Si	Cu	Cr	Fe	Mn	Ti	Al
wt%	0.93	0.52	0.19	0.10	0.29	0.10	0.02	Balance

2.2. CR Procedure

Plates with 200 mm width are annealed at 525 °C for 2 h to obtain a homogenous solid solution. Then, the samples are quenched in cold water to achieve a supersaturated solid solution. After solid solution treatment (SST), the samples are kept in liquid nitrogen (LN2) for 15 min, and their thickness is reduced from 10 mm to 1 mm in 15 rolling passes. Thickness reduction per pass is about 5%. The samples are kept in LN2 for 5 min after the fourth, eighth, and fourteenth pass. The diameter of the rolls is about 600 mm, and their speed is about 10 rpm. A schematic representation of the process is shown in Figure 1.
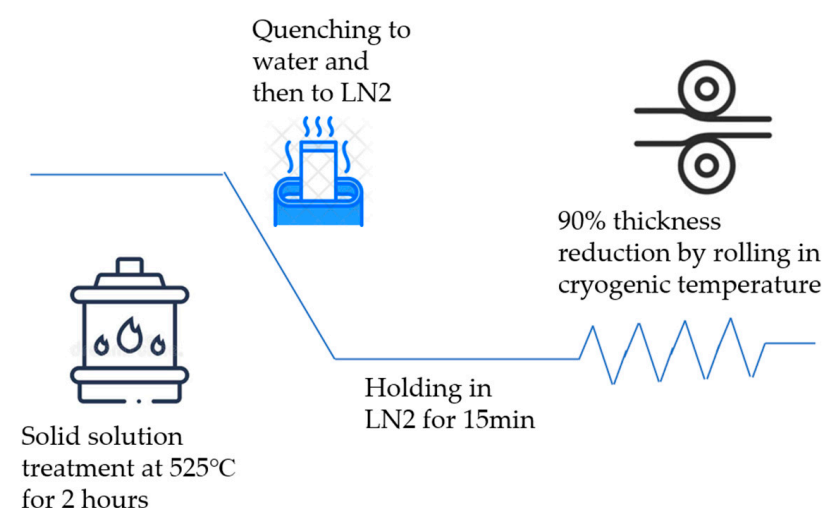
Figure 1. A schematic representation of solid solution treatment and cryogenic rolling.

2.3. Heat Treatment

After the CR procedure, the samples are subjected to an artificial aging treatment. For precipitation of the intermetallic β″ strengthening phase, artificial aging temperatures are chosen up to 150 °C because, at higher temperatures, the β″ phase can be converted

to more stable phases of β′ and β, which results in strength reduction. Consequently, in the present work, 100, 125, and 150 °C are chosen as the aging temperatures that should precipitate the beneficial GP zones and β″ phase [14,16]. Since it is highly challenging to characterize the exact type of precipitate structure in the severely deformed microstructure, both structures are denoted as strengthening precipitates in the following.

The samples are aged for 25 and 50 h at each temperature. Table 2 summarizes the applied heat treatment schedules.

Table 2. Sample preparation method.

Name	Aging Temperature	Aging Time/Hours
CR	-	-
100A	100 °C	25
100B	100 °C	50
125A	125 °C	25
125B	125 °C	50
150A	150 °C	25
150B	150 °C	50

2.4. Tensile Test

The tensile specimens are prepared by water-jet cutting based on the ASTM-E8 standard. The samples are cut parallel, 45°, and perpendicular to the rolling direction for each aging condition, as shown in Figure 2. Each test is conducted three times to validate the repeatability of the test result. The uniaxial tensile tests are performed at room temperature with the STM 20 Santam universal testing machine under ISO 7500 and a crosshead speed of 0.03 mm/s. Therefore, the initial strain rates are 0.003/s.
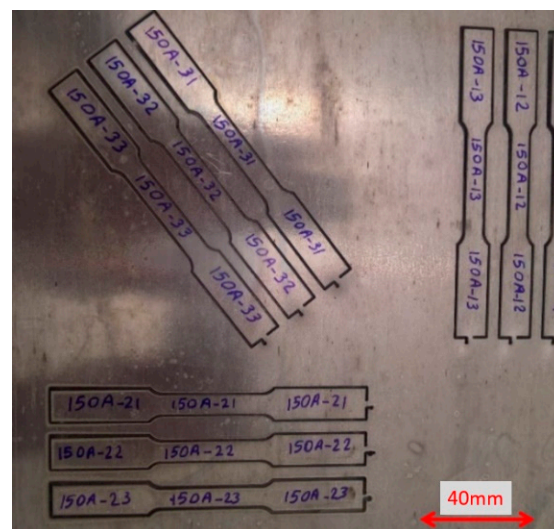
Figure 2. Tensile test samples cut in 0, 45°, and perpendicular to the rolling direction.

2.5. FLD Test

To evaluate forming limit diagrams (FLDs) according to the Nakajima test, ISO 12004 recommends a die with a semi-hemispherical punch, as shown in Figure 3. The radius of the hardened steel punch is 99 mm with a polished surface and a die diameter of 105 mm. A serrated blank holder is used to prevent the draw-in of the material.
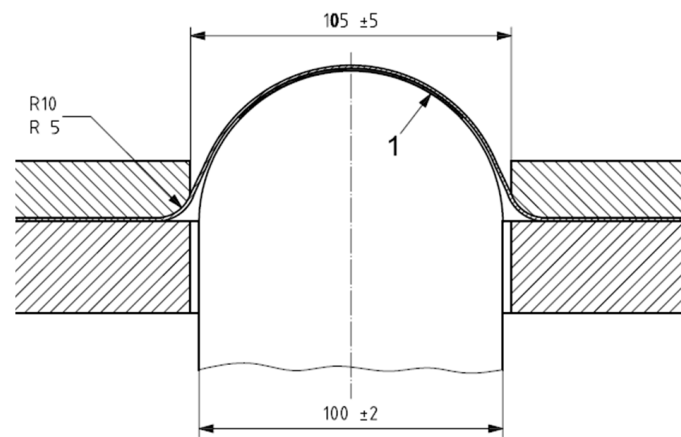
Figure 3. Illustration of the cross-section of the used tool (dimensions are in mm). The image is from ISO 12004.

Figure 4 shows the blanks for the FLD test. Five geometries are prepared to evaluate different strain regimes from uniaxial to biaxial tension. As recommended by ISO 12004 2, the water jet cutting process is used to prepare the samples to avoid cracks, work hardening, or microstructure changes. Therefore, the fracture does not initiate from the edge of the test pieces. For each geometry, the forming limit test is performed three times. In each test piece, circles with a diameter of 2.3 mm and squares with an edge of 2.5 mm are electrochemically etched to evaluate strains after deformation.
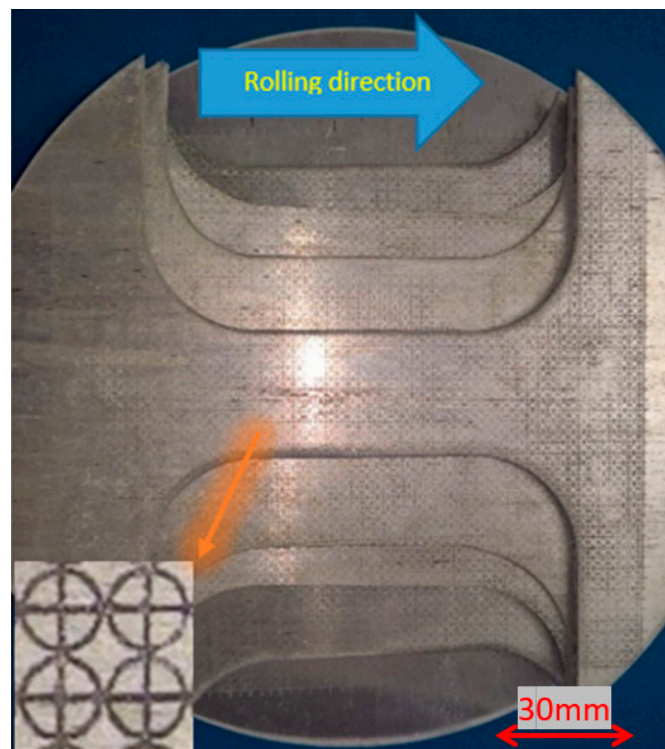
Figure 4. Blanks of FLD test pieces according to rolling direction; the blank width dimensions are 30, 70, 90, 120, and 185 mm.

A hydraulic press with a speed of about one mm/s is used to form the samples until a crack appears. Nylon and oil are applied between the punch and the test piece as a lubricant to achieve cracks near the dome's apex, as depicted in Figure 5.
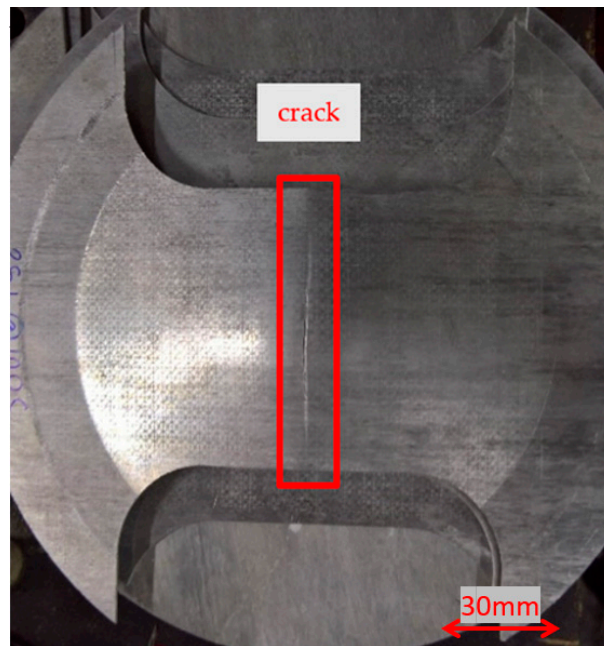
Figure 5. Deformed test pieces of forming limit diagram test. Cracks appear near the apex of the dome.

For each sample, circles are measured by a digital microscope with 60× magnification after a crack appears. Data are recorded after measurements. From the calculated strains, FLDs are constructed.

3. Results

The goal of the suggested method is to achieve a good balance of strength and formability. Since rolling can affect the properties of the material in different directions, the stress-strain curves for the samples in the rolling direction, diagonal, and transverse to the rolling direction at room temperature are presented in Figure 6.
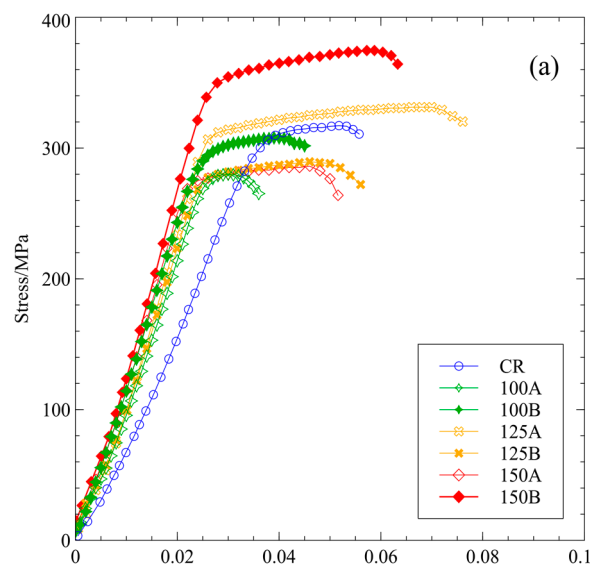
Figure 6. *Cont.*
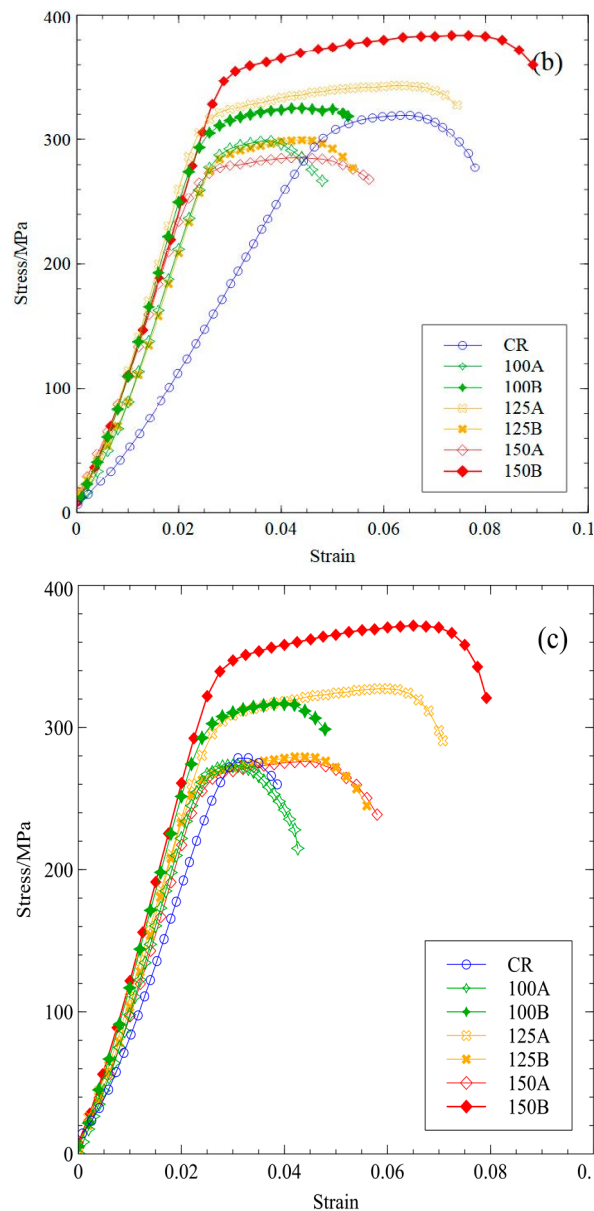
Figure 6. Stress-strain curve of samples (**a**) parallel to, (**b**) 45° to, and (**c**) perpendicular to the rolling direction.

For illustration, strain-hardening exponent n, (from $\sigma = C\varepsilon^n$) at plastic deformation is shown in Table 3. The strain-hardening is calculated according to ISO 10275 and is consistent with Yuan et al.'s [8,9] results. High strain-hardening results in less strain localization and uniform thickness distribution.

Table 3. Strain-hardening exponent n of plastic deformation for cryogenic rolled AA6061 in different heat treatment conditions.

Direction	CR	100A	100B	125A	125B	150A	150B
rolling	0.147	0.136	0.119	0.118	0.103	0.096	0.126
diagonal	0.209	0.130	0.132	0.130	0.136	0.112	0.135
transverse	0.388	0.131	0.127	0.127	0.115	0.111	0.131

Figure 7 summarizes the FLD for different aging treatments. Considering a slight difference in composition and process, the FLD of the CR sample is consistent with the study from Chandra Sekhar et al. [30]. The stress-strain curves show that the material has the

least strength and toughness in the CR condition. However, superior strength is achieved after aging treatment for 50 h at 150 °C. According to the FLDs, the best formability is observed at higher temperatures of age hardening. An increase in age hardening time also results in higher elongation to fracture.
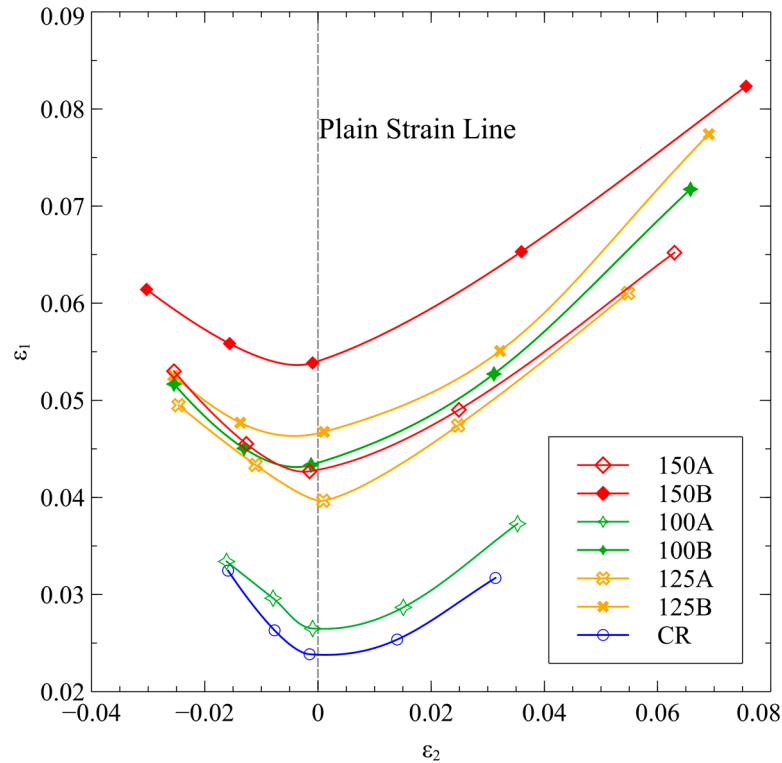
Figure 7. The forming limit diagram for different aging treatments of Aluminum Alloy 6061.

4. Discussion

The strength of cryogenic rolled material is affected by precipitation and dislocation density. Since these factors depend on time and temperature, heat treatment is essential. There is a difference in elastic modulus between CR and other samples. During cryogenic deformation, an extremely high dislocation density is introduced into the material, according to the balance between the generation of new mobile dislocations and annihilation by dynamic recovery as determined by the material's behavior at cryogenic temperatures. The very high dislocation density is not stable, however, at the higher temperature, where the tensile tests are performed. During the test, dynamic recovery and annihilation of dislocations will occur already at low stresses and dominate the plastic response of the material. This process overlays with the elastic response of the material and, consequently, changes the slope of the stress-strain curve at the beginning of the test. Apparently, this effect is also a strong function of the testing direction, as shown in Figure 6.

The strength of the CR samples is higher than that in the solid solution treated condition because of finer grain sizes after CR. Also, following the Taylor equation written below, the very high dislocation density after cryogenic rolling results in higher strength [31].

$$\sigma_y = \alpha M G b \sqrt{\rho} \tag{1}$$

where α is the strengthening coefficient, M is the Taylor factor, G is the shear modulus, b is the length of the burgers vector, and ρ is the density of dislocations. Suppression of dynamic aging and dynamic recovery during cryogenic rolling results in precipitate-free and ultra-fine grains with high dislocation density [17]. However, the matrix of the cryo-rolled samples corresponds to a supersaturated solid solution, where the precipitation of secondary phases depends on time and temperature. It is assumed that precipitation

does not occur at the cryogenic temperature due to the very low mobility of atoms under these conditions.

At test temperatures, static recovery of dislocations in heat-treated samples can reduce the strength. At the same time, some strengthening precipitates can form and increase the strength. Consequently, the difference in strength between CR and 100A should not be too much. The reason for lower strength in 125B and 150A can be attributed to the difference in hardening phases, but this would require further investigations of the microstructure, which are extremely difficult in highly deformed materials conditions, and therefore not performed here.

The age hardening treatment at 100 °C for 25 h does not significantly affect the CR samples, but aging for 50 h (100B) slightly increases strength and formability due to precipitation hardening and recovery [17].

For the 125A sample, there is a relatively good increase in formability and strength due to the recovery and formation of strengthening precipitates. However, as aging time increased (125B), the strength of the sample decreased again, while formability increased. Authors suggest that this behavior can be attributed to the annihilation of GP zones and reduction of the precipitate density, as well as decreasing dislocation density during recovery.

During aging at 150 °C, the β'' phase is assumed to be the primary strengthening precipitate. The 150A and 150B samples show good formability due to recovery and dislocation density reduction. After 25 h, a small amount of precipitation occurs and, therefore, a slight increase in strength is observed. For the 150B samples, the strength reaches its maximum due to more precipitation. These findings are consistent with Huang et al.'s [14] results. In their work, a DSC analysis is carried out at a heating rate of 10 °C/min for evaluating the precipitation sequences. In the current study, precipitation occurs already at lower temperatures due to the isothermal aging condition.

Solid solution treatment is carried out at 525 °C. There is no phase diagram for the exact chemical composition of the tested material available, but, according to thermodynamic simulation with Calphad databases [32,33], which gives a rough approximation, more than 70% of the nominal Mg and Si remain dissolved in the solid solution treatment. Consequently, the amount of Mg and Si in the matrix, which is available for precipitation hardening, is calculated to be more than 0.76 and 0.32 weight-%, respectively. Although not explicitly characterized in the present study, the work of Huang et al. [14] suggests that the main hardening precipitates in 100 °C and 125 °C aged samples are GP zones plus β''. Simultaneously, the primary hardening precipitate of 150 °C aged samples is expected to be predominantly β''. Precipitation is controlled by diffusion, which means that it occurs faster at higher temperatures. Furthermore, the highest rate of forming GP zones in cryo-rolled samples should be reached at about 125 °C, and the highest rate of forming β'' phase should be reached at about 150 °C, but it needs less time to reach its peak point. According to the FLD, a superior balance of strength and formability is achieved at 50 h of aging at 150 °C, resulting from a higher amount of hardening precipitates and lower dislocation density.

5. Conclusions

The present paper provides forming limits at room temperature for cryogenic rolled AA6061 after artificial aging at temperatures from 100 to 150 °C. The main conclusions of this work can be summarized as follows:

- The density of dislocations decreases during artificial aging due to static recovery. The second phase can also precipitate more easily due to enhanced diffusion. The formability of the material is improved by increasing the aging temperature or aging time. The strain-hardening coefficient shows that the reason for better formability can be the recovery, i.e., the reduction and rearrangement of dislocations.
- Aging at 150 °C for 50 h provides the best formability for different loading conditions, especially for tension-tension loading. The minor strain range is increased from 0.05 to 0.1, providing higher flexibility for multi-axial forming processes.

- The strength of the material is improved by 40%. The original value of 250 MPa for the cryogenic rolled sample increases to 350 MPa after 50 h of aging at 150 °C.

Author Contributions: A.S.; investigation, writing—original draft preparation, F.R.B.; supervision, E.K.; writing—review and editing and supervision. All authors have read and agreed to the published version of the manuscript.

Funding: This research received no external funding.

Data Availability Statement: Not applicable.

Acknowledgments: The authors would like to express their gratitude to Tomasz Wojcik from the Institute of Materials Science and Technology of TU Wien.

Conflicts of Interest: The authors declare no conflict of interest.

References

1. Smith, W.F. *Structure and Properties of Engineering Alloys*; McGraw-Hill, Inc.: New York, NY, USA, 1993; ISBN 0070585601.
2. Tenorio, J.A.S.; Espinosa, D.C.R. Recycling of Aluminum. In *Handbook of Aluminum*; Marcel Dekker, Inc.: New York, NY, USA, 2003; pp. 115–154, ISBN 0-07-059172-5.
3. Nageswara Rao, P.; Singh, D.; Jayaganthan, R. Effect of Annealing on Microstructure and Mechanical Properties of Al 6061 Alloy Processed by Cryorolling. *Mater. Sci. Technol.* **2013**, *29*, 76–82. [CrossRef]
4. Jandaghi, M.R.; Pouraliakbar, H.; Khalaj, G.; Khalaj, M.J.; Heidarzadeh, A. Study on the Post-Rolling Direction of Severely Plastic Deformed Aluminum-Manganese-Silicon Alloy. *Arch. Civ. Mech. Eng.* **2016**, *16*, 876–887. [CrossRef]
5. Vendra, S.S.L.; Goel, S.; Kumar, N.; Jayaganthan, R. A Study on Fracture Toughness and Strain Rate Sensitivity of Severely Deformed Al 6063 Alloys Processed by Multiaxial Forging and Rolling at Cryogenic Temperature. *Mater. Sci. Eng. A* **2017**, *686*, 82–92. [CrossRef]
6. Fritsch, S.; Scholze, M.; Wagner, M.F.X. Influence of Thermally Activated Processes on the Deformation Behavior during Low Temperature ECAP. *IOP Conf. Ser. Mater. Sci. Eng.* **2016**, *118*, 012030. [CrossRef]
7. Korznikov, A.V.; Mulyukov, R.R.; Valiev, R.Z. Structure and Properties of Ultrafine-Grained Materials Produced by Severe Plastic Deformation. *Mater. Sci. Eng. A* **1993**, *168*, 141–148.
8. Yuan, S.; Cheng, W.; Liu, W. Cryogenic Formability of a Solution-Treated Aluminum Alloy Sheet at Low Temperatures. *J. Mater. Process. Technol.* **2021**, *298*, 117295. [CrossRef]
9. Yuan, S.; Cheng, W.; Liu, W.; Xu, Y. A Novel Deep Drawing Process for Aluminum Alloy Sheets at Cryogenic Temperatures. *J. Mater. Process. Technol.* **2020**, *284*, 116743. [CrossRef]
10. Dong, F.; Huang, S.; Yi, Y.; Wang, B.; He, H. Flow Behaviors and Deformation Mechanism of WQ-Tempered Al–Li Alloy at Cryogenic Temperatures. *Mater. Sci. Eng. A* **2021**, *809*, 140971. [CrossRef]
11. Magalhães, D.C.C.; Kliauga, A.M.; Sordi, V.L. Flow Behavior and Fracture of Al−Mg−Si Alloy at Cryogenic Temperatures. *Trans. Nonferrous Met. Soc. China* **2021**, *31*, 595–608. [CrossRef]
12. Liu, Y.; Zhao, X.; Li, J.; Bhatta, L.; Luo, K.; Kong, C.; Yu, H. Mechanical Properties of Rolled and Aged AA6061 Sheets at Room-Temperature and Cryogenic Environments. *J. Alloys Compd.* **2021**, *860*, 158449. [CrossRef]
13. Singh, D.; Nageswara Rao, P.; Jayaganthan, R. Microstructures and Impact Toughness Behavior of Al 5083 Alloy Processed by Cryorolling and Afterwards Annealing. *Int. J. Miner. Metall. Mater.* **2013**, *20*, 759–769. [CrossRef]
14. Huang, Y.C.; Yan, X.Y.; Qiu, T. Microstructure and Mechanical Properties of Cryo-Rolled AA6061 Al Alloy. *Trans. Nonferrous Met. Soc. China* **2016**, *26*, 12–18. [CrossRef]
15. Satish, D.R.; Feyissa, F.; Kumar, D.R. Cryorolling and Warm Forming of AA6061 Aluminum Alloy Sheets. *Mater. Manuf. Process.* **2017**, *32*, 1345–1352. [CrossRef]
16. Rao, P.N.; Panigrahi, S.K.; Jayaganthan, R. Effect of Annealing and Aging Treatment on Mechanical Properties of Ultrafine Grained Al 6061 Alloy. *Mater. Sci. Technol.* **2010**, *26*, 371–374. [CrossRef]
17. Panigrahi, S.K.; Devanand, D.; Jayaganthan, R. Effect of Ageing on Strength and Ductility of Ultrafine Grained Al 6061 Alloy. *Mater. Sci. Forum* **2010**, *633–634*, 303–309. [CrossRef]
18. Rangaraju, N.; Raghuram, T.; Krishna, B.V.; Rao, K.P.; Venugopal, P. Effect of Cryo-Rolling and Annealing on Microstructure and Properties of Commercially Pure Aluminium. *Mater. Sci. Eng. A* **2005**, *398*, 246–251. [CrossRef]
19. Izumi, M.T.; Quintero, J.J.H.; Crivoi, M.R.; Maeda, M.Y.; Namur, R.S.; de Aguiar, D.J.M.; Cintho, O.M. In Situ X-Ray Diffraction Analysis of Face-Centered Cubic Metals Deformed at Room and Cryogenic Temperatures. *J. Mater. Eng. Perform.* **2019**, *28*, 4658–4666. [CrossRef]
20. Sarma, V.S.; Wang, J.; Jian, W.W.; Kauffmann, A.; Conrad, H.; Freudenberger, J.; Zhu, Y.T. Role of Stacking Fault Energy in Strengthening Due to Cryo-Deformation of FCC Metals. *Mater. Sci. Eng. A* **2010**, *527*, 7624–7630. [CrossRef]
21. Lee, W.S.; Huang, Y.C. Mechanical Properties and Dislocation Substructure of 6061-T6 Aluminum Alloy Impacted at Cryogenic Temperatures. *Mater. Trans.* **2016**, *57*, 344–350. [CrossRef]

22. Changela, K.; Krishnaswamy, H.; Digavalli, R.K. Development of Combined Groove Pressing and Rolling to Produce Ultra-Fine Grained Al Alloys and Comparison with Cryorolling. *Mater. Sci. Eng. A* **2019**, *760*, 7–18. [CrossRef]

23. Wang, X.; Fan, X.; Chen, X.; Yuan, S. Cryogenic Deformation Behavior of 6061 Aluminum Alloy Tube under Biaxial Tension Condition. *J. Mater. Process. Technol.* **2022**, *303*, 117532. [CrossRef]

24. Rao, P.N.; Kaurwar, A.; Singh, D.; Jayaganthan, R. Enhancement in Strength and Ductility of Al-Mg-Si Alloy by Cryorolling Followed by Warm Rolling. *Procedia Eng.* **2014**, *75*, 123–128. [CrossRef]

25. Taye, F.; Das, P.; Kumar, D.R.; Sankar, B.R. Characterization of Mechanical Properties and Formability of Cryorolled Aluminium Alloy Sheets. In Proceedings of the 5th International and 26th All India Manufacturing Technology, Design and Research Conference (AIMTDR 2014), Guwahati, India, 12–14 December 2014; Volume 511, pp. 1–5.

26. Cavusoglu, O.; Leacock, A.G.; Gürün, H. Forming-Limit Diagrams and Strain-Rate-Dependent Mechanical Properties of AA6019-T4 and AA6061-T4 Aluminium Sheet Materials. *Mater. Tehnol.* **2016**, *50*, 1005–1010. [CrossRef]

27. Kumar, M.; Sotirov, N.; Grabner, F.; Schneider, R.; Mozdzen, G. Cryogenic Forming Behaviour of AW-6016-T4 Sheet. *Trans. Nonferrous Met. Soc. China* **2017**, *27*, 1257–1263. [CrossRef]

28. Barfeh, A.; Hashemi, R.; Safdarian, R.; Rahmatabadi, D.; Aminzadeh, A.; Sattarpanah Karganroudi, S. Predicting the Forming Limit Diagram of the Fine-Grained AA 1050 Sheet Using GTN Damage Model with Experimental Verifications. *Proc. Inst. Mech. Eng. B J. Eng. Manuf.* **2022**, 095440542211389. [CrossRef]

29. Wang, C.; Yi, Y.; Huang, S.; Dong, F.; He, H.; Huang, K.; Jia, Y. Experimental and Theoretical Investigation on the Forming Limit of 2024-O Aluminum Alloy Sheet at Cryogenic Temperatures. *Met. Mater. Int.* **2021**, *27*, 5199–5211. [CrossRef]

30. Chandra Sekhar, K.; Narayanasamy, R.; Venkateswarlu, K. Formability, Fracture and Void Coalescence Analysis of a Cryorolled Al-Mg-Si Alloy. *Mater. Des.* **2014**, *57*, 351–359. [CrossRef]

31. Yadollahpour, M.; Hosseini-Toudeshky, H.; Karimzadeh, F. Effect of Cryorolling and Aging on Fatigue Behavior of Ultrafine-Grained Al6061. *JOM* **2016**, *68*, 1446–1455. [CrossRef]

32. Povoden-Karadeniz, E.; Lang, P.; Warczok, P.; Falahati, A.; Jun, W.; Kozeschnik, E. CALPHAD Modeling of Metastable Phases in the Al–Mg–Si System. *Calphad* **2013**, *43*, 94–104. [CrossRef]

33. Harals, F.; Gödecke, T.; Lukas, H.L.; Sommer, F. Investigation of the Al-Mg-Si System by Experiments and Thermodynamic Calculations. *J. Alloys Compd.* **1997**, *247*, 31–42.